CERN/SPSC/99-27
SPSC/P309 ADD.1
August 24, 1999

Memorandum. Addendum to P309 and request for beam time in 2000.

Mikhail Dubrovin, Vladimir Golubev, Vladimir Strakhovenko, Viacheslav Shary *
Budker Institute of Nuclear Physics, Novosibirsk, Russia

Xavier Artru, Michel Chevallier
Institut de Physique Nucléaire, Lyon, France

Robert Chehab
Laboratoire Accélérateur Linéaire, Orsay, France

Abstract

This memorandum is concerning the Track Reconstruction in the positron detector of P309 and the requested beam time. The positron detector is a Drift Chamber filled with He and CH4 (10%) and partially inserted in a magnetic field parallel to the wires. It consists of two independent parts DC1 and DC2 residing in the common gas volume. DC1 is outside the magnetic field, whereas DC2 is in the region of uniform magnetic field. The Track Reconstruction method used for each part is described: it is essentially based on the histogramming method with an angular parameter (K) for DC1, where straight lines are expected, and a curvature parameter (C) for DC2, where the trajectories are circular. An optimal track is found by a fitting procedure, which is described. The results of the calculations are concerning the distributions of the deviations of the reconstructed tracks from the simulated tracks, with respect to the two parameters K and C, the rates of reconstructed and false tracks over accepted tracks, and comparisons between simulated, accepted, reconstructed and false tracks. Some examples of simulated and reconstructed tracks are also presented. Most of the simulations are related to crystal targets. Some simulations with amorphous targets, where the lower rate of occupancy makes the reconstruction less critical "a priori", are also presented. The influence of finite dimensions beams is also considered. The main conclusion of the track reconstruction shows that the reconstruction efficiency is higher than 60% in the region of high occupancy and nearly 95% in the larger part of the detector. The beam time requests are concerning, in addition to the necessary week for calibration and tests, two weeks of data taking for which the first one, will be mainly devoted to relative measurements. A status of the positron and photon detectors is also given.

*e-mail: V.V.Shary@inp.nsk.su

1 Introduction

A proposal for an experiment concerning a positron source using channeling of ultrarelativistic electrons in a tungsten crystal has been presented at the January (99) session of the SPSC. This experiment is supposed to be installed on the transfer lines X5 or X7 of the SPS. The positron detector is essentially based on a Drift Chamber partially inserted in a magnetic field. In the first part (before the magnetic field) as in the second part (inside the magnetic field) the rate of occupancy in the cells is rather high, especially near the propagation axis. Such situation could lead, "a priori", to a difficult reconstruction task for the positron trajectories. The purpose of this work, presented hereafter, is to study the track reconstruction in the whole Drift Chamber. Monte-Carlo simulations have been worked out with a low energy Cut-Off ($\sim 1\ MeV$). Precisions are also given on the status of the experimental apparatus as on the measurement programme, which has been optimized.

A Track reconstruction in the magnetic spectrometer for the channeling experiment.

A.1 The choice of the track reconstruction method.

The main part of the detector for the channeling experiment [1] is the drift chamber for the positron detection, which consists of two parts: first part (DC1) and second part (DC2) located in the magnetic field. The set-up is represented w.r.t. a three-dimensional axis frame where X corresponds to the beam propagation axis, Y, the axis perpendicular to it in the horizontal plane and Z, the vertical axis. The parameter K is the angle between the trajectory and the axis X ($K = P_Y/P_X$).

The cell occupancy near the beam direction is very high (see fig. 1; on figure 2 the track multiplicity in parts 1,2 is shown). Hence, the efficiency in each layer will be small. In these conditions using any local track recognition method will be inefficient, so the histogramming method has been chosen [2, 3].

The total scheme of track reconstruction looks like:

1. the track recognition in the first part (straight line);
2. the track fitting in the first part with the assumption that the impact parameter, distance from the track to the centre of the target, is equal to zero;
3. the track recognition in the second part (constant curvature);
4. the total track fitting

In order to test the reconstruction program 10000 events were used with a new event generator using a total energy cutoff of 1.1 MeV.The target thickness is $8mm$. The positron point source was considered.

A.2 The tracks finding in DC1.

For the tracks finding in the DC1 chamber the standard histogram method has been used [2]. The tracks are parametrised as $y = K \cdot x$. For each hitted cell two "mirror" values for the K parameter are calculated:

$$K_{i\,\pm} = \frac{(y_i - y_t)\sqrt{(x_i - x_t)^2 + (y_i - y_t)^2 - r_i^2} \mp r_i(x_i - x_t)}{(x_i - x_t)\sqrt{(x_i - x_t)^2 + (y_i - y_t)^2 - r_i^2} \pm r_i(y_i - y_t)},$$

where x_t, y_t represent the centre of the target position, x_i, y_i the wire coordinates, r_i the measured distance from the wire to the track.

The histogram on K parameter is built. If both "mirror" values for a hitted cell are in the same bin they are counted once. The bin with the highest number of counts is found, this bin represent a track and track parameter K is equal to the centre of this bin. After this, all counts of the cells attached to the track are removed from the histogram and the track finding procedure is repeated until the number of the hits in each bin is smaller than 3. If the real track comes near a bin boundary in that case some of the cell hits can appear in a neighbouring bin and the number of counts in this bin will decrease. To suppress this effect two histograms on parameter K are used. The bin position of the second histogram is shifted by half a bin with respect to the first histogram. The track finding procedure works simultaneously with the two histograms. The bin size was chosen to be $dK = 0.0035$ which correspond to the uncertainty in the impact parameter $db \sim 1mm$. After track finding in DC1, a new K parameter is determined for each track using least squares method with assumption that all tracks come from the centre of the target (x_t, y_t). The fig. 3 shows the accuracy on K parameter. Some results on the track reconstruction in DC1 are presented on figures 4–7.

The notation used on the pictures is the following:

1. N_{ACC} — number of *accepted* tracks by the DC1 or DC2. The track is called *accepted by DC1(DC2)* if the event is *accepted* and if a minimum of 3 (4) cells are hitted by this track. An event is called *accepted* if any track in this event fired the DC counters. The DC counters are located on two lateral walls of the drift chamber and limit its vertical acceptance to the zone of homogeneous electric field (as resulting from tests and simulations): their height is of 3 cm.

2. N_{REC} — number of *reconstructed* tracks. The track is called *reconstructed* in DC1 if the difference between the reconstructed parameter K_{REC} and the simulated one K_{SIM} is smaller than 0.01. The track is called *reconstructed* in DC2 if the difference between the reconstructed curvature C_{REC} and the simulated one C_{SIM} is smaller than 0.003. The difference between *accepted* and *reconstructed* tracks represents the *lost* (not reconstructed) tracks.

3. N_{FALSE} — number of the *false* track. The track is *false* in DC1 if the difference between the reconstructed parameter K_{REC} and the simulated parameter K_{SIM} of the nearest track is larger than 0.01. The track is *false* in DC2 if the difference between the reconstructed curvature C_{REC} and the simulated one C_{SIM} of the nearest track is larger than 0.003.

A.3 The track finding in DC2.

In the second part of the drift chamber the particle tracks represent arcs with curvatures which depend on the particle momentum as $C = \frac{3 \cdot 10^{-4} B}{\sqrt{p_x^2 + p_y^2}}$, where B is the magnetic field in *Gauss*, p_x, p_y are the projections of the particle momentum in MeV/c on the axes X,Y , C is the track curvature in cm^{-1}. The arc position depends on the track angle and the y-coordinate of the track entrance point in the second part which can be expressed as $y = Kx_m$, where x_m is the distance between the centre of the target and the magnetic field boundary. So the track model has two parameters: $K = tg\alpha$, where α is the angle between the track and the X-axis and C which is the curvature of the track.

For track finding in the second part of the drift chamber, the histogram method is used. For each track reconstructed in the first part of the drift chamber, the histogram on the curvature is built. The curvature for the track with the parameter K and cell i is calculated as

$$C_{\pm} = \frac{\frac{Kx_i - y_i}{\sqrt{1+K^2}} \pm r_i}{(x_i - x_m)^2 + (y_i - Kx_1)^2 - r_i^2},$$

where x_i, y_i is the wire coordinate, r_i is the measured distance from wire i to the track. Two curvatures, C_+, C_- correspond to "mirror" values which are possible for the reconstructed track.

The accuracy on the K parameter determination was taken into account, so the bin C_0 is filled if the hit lies between the tracks with parameters $(K_0 - dK, C_0 - dC)$ and $(K_0 + dK, C_0 + dC)$. These parameters were chosen for DC2: $2 \cdot dK = 3.25 \cdot 10^{-3}$, $2 \cdot dC = 4 \cdot 10^{-4}$.

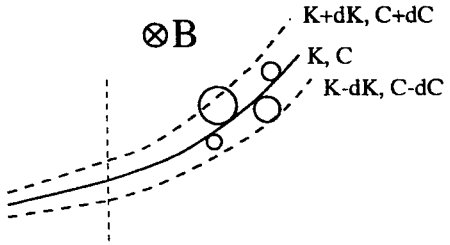

In order to reconstruct the tracks which are not detected in DC1, we build a two-dimensional histogram (in K and C) after having divided the K domain between -0.06 and 0.20 into 80 bins. Each bin in the (K,C) histogram (with widths $2 \cdot dK = 3.25 \cdot 10^{-3}$ and $2 \cdot dC = 4 \cdot 10^{-4}$) represents a track-candidate. To be considered as a real track, the track-candidate must have a number of counts larger than a threshold fixed at 4. Then we choose the bin with the highest number of counts. This bin represents the first track. As any hit can give a contribution to different bins in the (K,C) histogram, we have to remove the counts associated to the first track before repeating the operation; that operation is repeated until the number of counts in every bin goes below the threshold.

For suppressing the cell bound effect described in section A.2, the second histogram on curvature with cell shifted on 1/2 cell size is produced for each value of the K parameter. The bin with the highest count between the two histograms is chosen as was done with parameter K.

Some results on the track reconstruction in DC2 are presented on figures 8–15. All results are presented only for positron tracks. On figures 14 and 15 different positron energy domains have been considered.

Several simulated and reconstructed events with high multiplicity are presented on the pictures 23–25. The solid frame indicates geometrical cuts for the particles because of the DC construction. The dashed frames indicate cells bounds (approximately). The dashed line divides the chamber into regions with/without magnetic field. The circles represent the hits in the DC cells. Particles signals are randomised using the normal distribution with a dispersion of 0.3 mm. If several signals from different particles hit the same cell the signal with the largest distance is registered (according to the TDC mode).

A.4 Track fitting.

The track in the drift chamber consists of two parts: a straight line and an arc. The straight line is described with the equation $y = Kx + b$, the arc is described with the curvature C and by the entrance point of the track in the magnetic field region with coordinate $(x_m, Kx_m + b)$, x_m being the distance from the centre of the target to the magnetic field region. The optimal track parameters were found by minimisation of the following quadratic form:

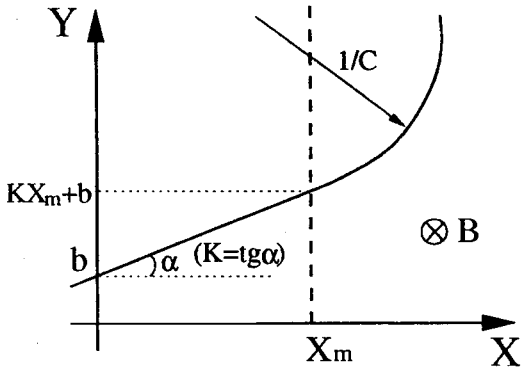

$$Q^2(\vec{p}) = \sum_{i=1}^{N_1+N_2} \sum_{j=1}^{N_1+N_2} (r_i - f_i(\vec{p})) \cdot W_{ij} \cdot (r_j - f_j(\vec{p})),$$

where $\vec{p}$ is the parameters vector (b,K,C), N1 is the number of the sensitive wires in the first part of the drift chamber, N2 is the number of the sensitive wires in the second part, r_i is the measured distance from wire i to the track, $f_i(\vec{p})$ is the calculated distance from the wire i to

the track with vector of parameters $\vec{p}$, which is equal to:

$$f_i(\vec{p}) = \pm(\frac{1}{C} - \sqrt{(x_i - x_m)^2 + (y_i - Kx_m - b)^2 + \frac{1}{C^2} + \frac{2}{C\sqrt{1+K^2}}(Kx_i + b - y_i)})$$

for the second part and

$$f_i(\vec{p}) = \mp\frac{Kx_i + b - y_i}{\sqrt{1+K^2}}$$

for the first part or for the case $C \to 0$, W_{ij} — weight matrix. The minimisation was done using Newton method [4]. We can write the Taylor series expansion of the Q^2 around some point $\vec{p}_0$ (on the first step $\vec{p}_0$ is given by track finding procedure):

$$Q^2(\vec{p}) = Q^2(\vec{p}_0) + \vec{g} \cdot (\vec{p} - \vec{p}_0) + \frac{1}{2} \cdot (\vec{p} - \vec{p}_0)^* \cdot G \cdot (\vec{p} - \vec{p}_0),$$

$$g_k = -2 \sum_{i,j}^{N_1+N_2, N_1+N_2} \frac{\partial f_i(\vec{p})}{\partial p_k}\Big|_{\vec{p}_0} \cdot W_{ij} \cdot (r_j - f_j(\vec{p}_0),$$

$$G_{kl} = 2 \sum_{i,j}^{N_1+N_2, N_1+N_2} \{\frac{\partial f_i(\vec{p})}{\partial p_k}\Big|_{\vec{p}_0} \cdot W_{ij} \cdot \frac{\partial f_j(\vec{p})}{\partial p_l}\Big|_{\vec{p}_0} - \frac{\partial^2 f_i(\vec{p})}{\partial p_k \partial p_l}\Big|_{\vec{p}_0} \cdot W_{ij} \cdot (r_j - f_j(\vec{p}_0)\}$$

After vector $\vec{g}$ and matrix G calculation, the new vector of parameters $\vec{p}$ is calculated as $\vec{p}_{new} = \vec{p}_0 - G^{-1} \cdot \vec{g}$ and then the fitting procedure is repeated until the convergence criteria will be fulfilled.

A.5 Amorphous target

In order to compare the amorphous target and the crystal a simulation involving 2000 events has been analysed. The target thickness is $8mm$, energy cutoff is $1.1MeV$, positron point source was considered. The results are presented on figures 16-22. The comparison between crystal and amorphous target shows that:

1. the DC occupancy is lower for the amorphous target.
2. the track multiplicity is lower for the amorphous target by a factor 1.5;
3. in the case of the amorphous target the track reconstruction procedure works also well or better than in the case of the crystal target;
4. the maximum in the energy spectrum is shifted for the amorphous target in comparison with the crystal towards $\sim 50MeV$: that corresponds to harder positrons than with a crystal target.

A.6 Some remarks on the beam size influence.

In order to take into account the electron beam size, the randomisation of the particles coordinates in Y,Z plane has been done with Gaussian distribution, R.M.S. = 1 mm. As was already seen, the number of the reconstructed tracks was improved using two-dimensional histogram in the K region defined in $[-0.06, 0.2]$. As this number is good enough, we have tried for the case of finite size of the beam to decrease the number of the false tracks, restricting the K domain to $[-0.06 \div 0.06]$ with very few consequences on the number of reconstructed tracks. Also, the bin size for the histogram in DC1 has been made larger from $dK = 0.0035$ to 0.005 and the bin size of the histogram in K parameter in DC2 has been increased from 0.00325 to 0.004. These changes allow to have a better track reconstruction capability if one takes into account the beam size. The results which have been obtained with 10000 events are presented on the figures 26–35. Making comparison with previous results one can conclude that:

1. the accuracy in K parameter is 3 times worse due to the uncertainty in the target interaction point (fig 26).

2. the ratio reconstructed/accepted tracks in DC1 does not change significantly (fig.27).

3. the ratio false/accepted tracks in DC1 increased by a factor 2, but the total number of false track is small, near 3% (fig. 28, 29).

4. the accuracy in the curvature did not change significantly (fig. 30).

5. the ratio reconstructed/accepted tracks in DC2 did not change significantly (fig. 31).

6. the number of the false track increased in the region with K parameter smaller then 0.06, but decreased in the region with $K > 0.06$ (fig. 32, 33,35 for the DC2) due to changes which have been done for the track reconstruction parameters (see above).

7. As one can see on fig. 35 the biggest contamination of the *false* tracks is in the energy domain 10-25 MeV. For decreasing the number of the *false tracks* the lower value of magnetic field (0.1 T) should be used in oder to get better results in this energy domain.

A.7 Some remarks on the ratio *false/reconstructed* tracks dependence on K parameter.

One can see that the ratio *false/accepted* tracks depends in different way in DC1 and DC2 from the K parameter. In DC2 this ratio depends in normal way, that means, that the ratio is decreased when the occupancy is decreased, this corresponds to the increasing K parameter. In DC1 the ratio *false/accepted* tracks is increased when the occupancy is decreased (the K parameter is increased). The possible explanation of this effect can be like this. In DC1 the drift chamber cells structure is aligned with the line which has a constant angle with beam axis 33.7° (see picture). If the track is parallel and close to this line, the false reconstruction has a large probability because of ambiguities in tracks direction for the cells measurement and the limited DC accuracy. Tracks which are coming through the cell which is far from the beam will be more parallel to the cell line than tracks which are coming through the cell near the beam line. That is why the tracks with big K parameter have larger probability of false reconstructing. There is no this kind of problems in DC2, because tracks are represented by circles, not by straight lines. In order to decrease the number of the false tracks in DC1, the changes in the tracks reconstruction algorithm, which allow to get better capability to resolve the ambiguities, will be done.

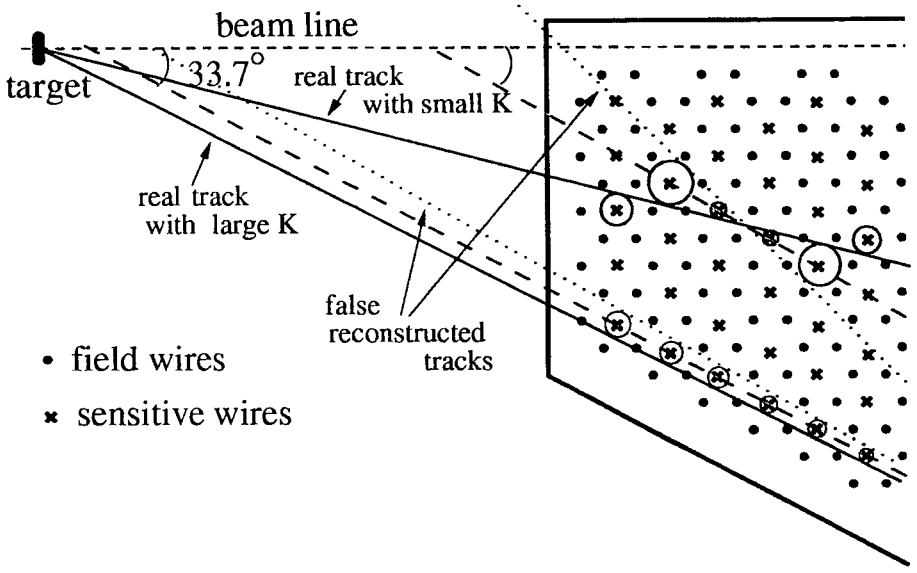

A.8 Conclusion.

The track reconstruction procedure based on the histogramming method was developed for the magnetic spectrometer in the channeling experiment. The tests of the reconstruction procedure have been done with the new generator with a cutoff of $1.1MeV$ for the crystal and the amorphous target. Though the occupancy is extremely high in the cells nearest to the beam the reconstruction procedure give quite good results: the reconstruction efficiency in the worse case (small angle, high occupancy) is near 60 % and near 95 % in the larger part of the detector volume (fig.4,9). The rate of the false tracks is quite low (fig.5,10). The two values of the magnetic field are necessary for covering all interesting energy domains. In the results presented above, the multiple scattering has not been taken into account. However, it has been estimated. The estimation of the uncertainty due to the multiple scattering gives the following numbers:

1. for the particle passage before drift chamber — 1mm
2. for the particle passage in drift chamber between cells — 100μ
3. for the particle passage between DC1 and DC2 — 1mm

These values do not affect the correct working of the reconstruction procedure and the influence of the multiple scattering can be taken into account in the fitting procedure.

Now, with the improved particles generator, it is possible to study the backgrounds with GEANT simulation and this will be done in the nearest future. Also the multiple scattering will be studied with simulation and some improvement in the reconstruction algorithm will be done in order to decrease the number of the false reconstructed tracks.

References

[1] X.Artru et al. NIM B **145** (1998) 221

[2] *H.Grote* Rep.Prog.Phys. **50** (1987) 473–500

[3] *H.Eichinger*, Nucl.Inst.Meth. **176** (1980) 417–424

[4] *H.Eichinger and M.Regler*, preprint CERN 81-06 (1981)

B Some precisions about the requested running time for the P309 proposal and on the status of the detection system.

The requested running time for the channeling experiment is precised as well as the status of construction of the detection system.

B.1 Programme of data taking for the channeling experiment.

The expected outputs from this experiment are:

- for the positrons: the yield, the spectrum and emittance (angular distribution),
- for the photons: the multiplicity and radiated energy.

The needed statistical precision is of 3%. Many parametrised histograms each of them having 50 bins on the average have to be constructed. Taking into account the number of triggered events (200/sec with a 1 mrad angular aperture) and the corresponding positron yields in given windows, as resulting from our simulations, we have estimated the number of runs based on the following procedure:

- two magnetic field values (0.1 and 0.4 Tesla) must be taken in order to cover enough the energy domain,
- the measurements must concern different values (6) of the rocking angle; this procedure will us allow to know the actual aperture angle where crystal effects are operating and to get, quite simply, the comparison between crystal and amorphous targets.

The simplified programme for the photons, for which the data taking will be simultaneous with that of the positrons, does not require additional runs.

On this basis, two weeks of data taking are necessary, after the test and calibration run (1 week) which is necessary to set up our detection system. The wished repartition is then:

1 week of test and calibration || m weeks interval || 1 week for data taking; relative measurements will be considered first, absolute also. || n weeks interval || 1 additional week of data taking, if the full detection system is working well and able to bring absolute informations with the needed precision. These weeks must not be consecutive but separated by some delays.

The removal of the Drift Chamber and of the Goniometer Chamber, to allow free space to others experiments in the same area, have been considered during the intervals of our runs. Such operation will require the use of the first day of the week of data taking to make rapid tests.

B.2 Status of the drift chamber construction.

The Drift Chamber construction has been completed in the Budker Institute in Novosibirsk, by end of July 99. Preliminary tests with the chamber filled with Argon and CO2(10%) and with 2 KVolts showed quite uniform response from wire to wire for the whole channels. The Chamber fully equipped with the external connectors will be sent to LAL-Orsay by this mid-October in order to be fully tested with the front-end electronics and the acquisition system before being sent to CERN.

B.3 Status of the photon detector.

The NaI crystal (Calorimeter) provided by BINP-Novosibirsk is in Tomsk for some tests. The Pre-Shower (Multiplicimeter) as the whole mechanical system for the photon detector is developed by the Kharkov team.

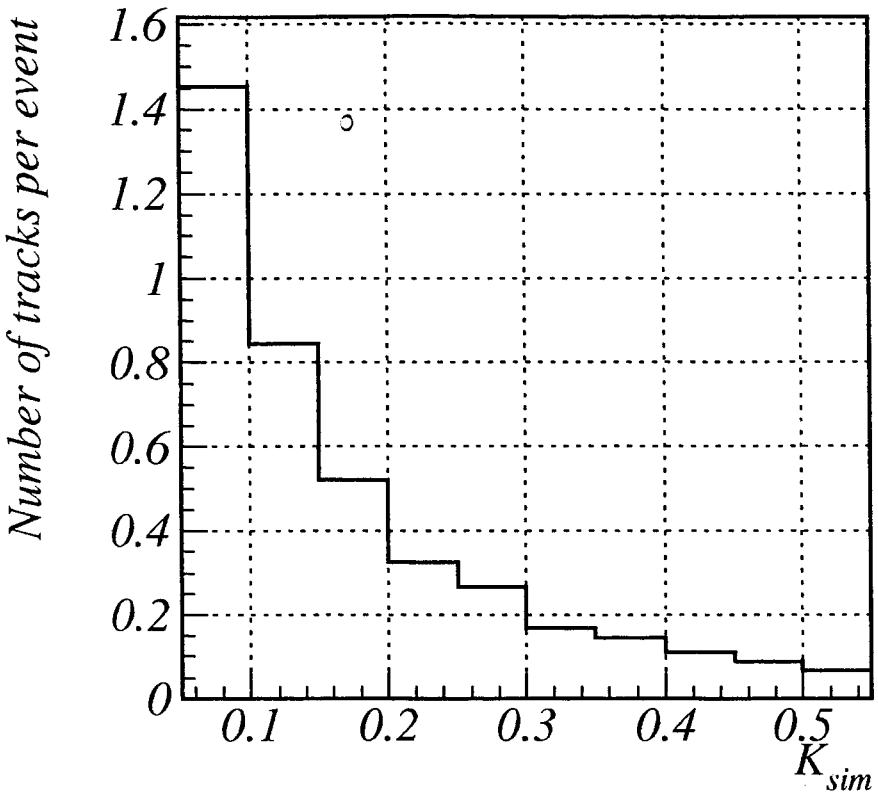

Figure 1: The dependence of the average number of accepted tracks per event in DC1 from K_{SIM}.

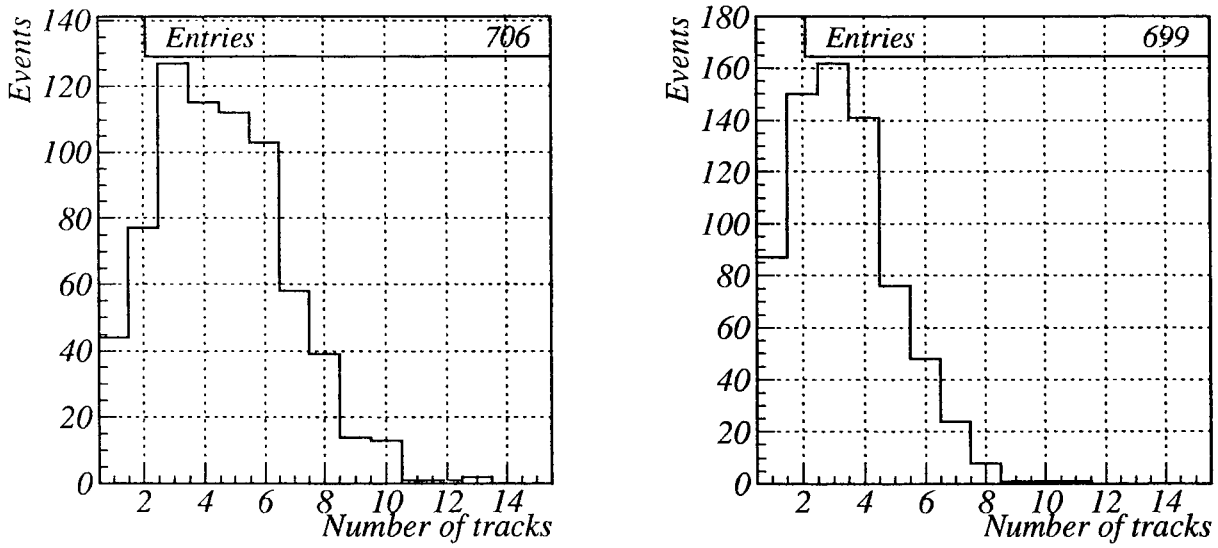

(a) first part

(b) second part

Figure 2: The tracks multiplicity of the tracks accepted (a) — in DC1, (b) — in DC2 with magnetic field $0.4T$.

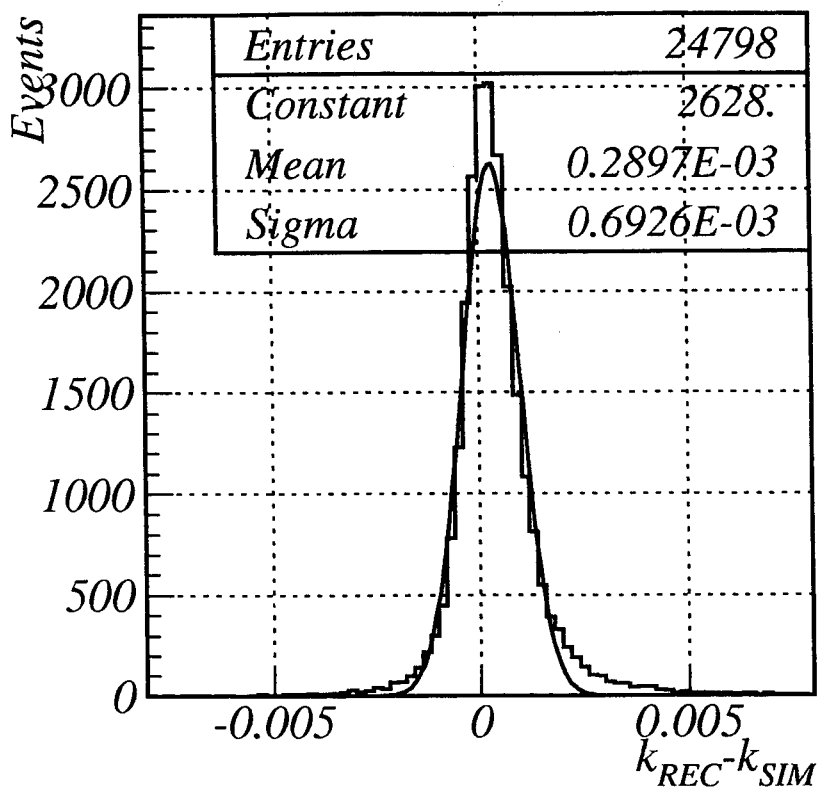

Figure 3: dK spectrum, where dK — difference between reconstructed K_{REC} and simulated one $K_{SIM} = P_Y/P_X$.

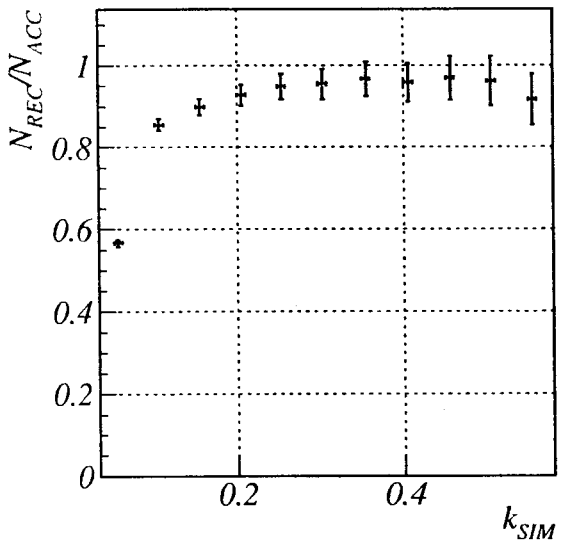

Figure 4: The ratio between reconstructed and accepted tracks in DC1.

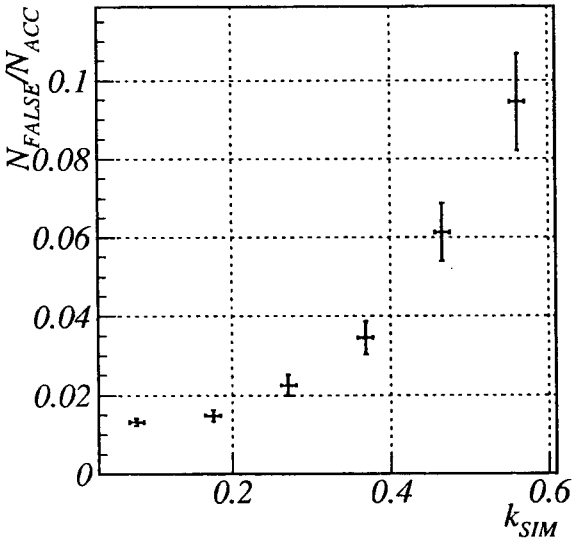

Figure 5: The ratio between false and accepted tracks in DC1.

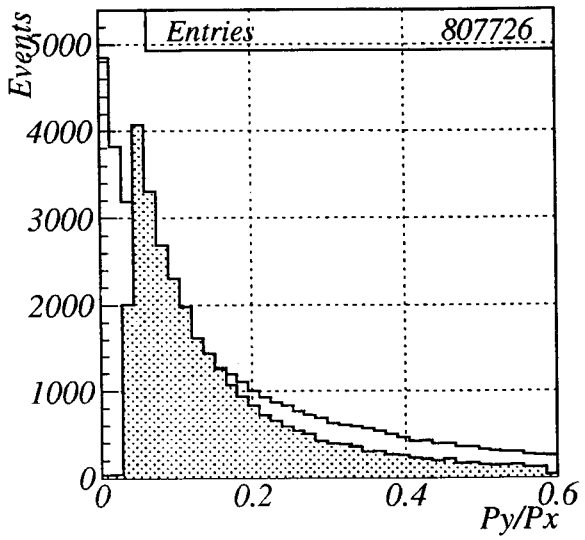

Figure 6: The unfilled histogram is the simulated tracks distribution on parameter K_{SIM} multiplied by the scaling factor 0.25 . The gray histogram is the accepted tracks in DC1.

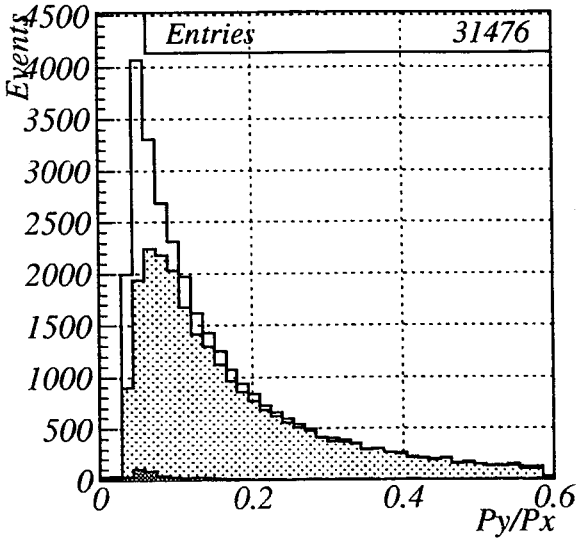

Figure 7: The unfilled histogram is the accepted tracks distribution on parameter K_{sim} in DC1. The gray histogram is the reconstructed tracks in DC1.The dark histogram is the false tracks in DC1.

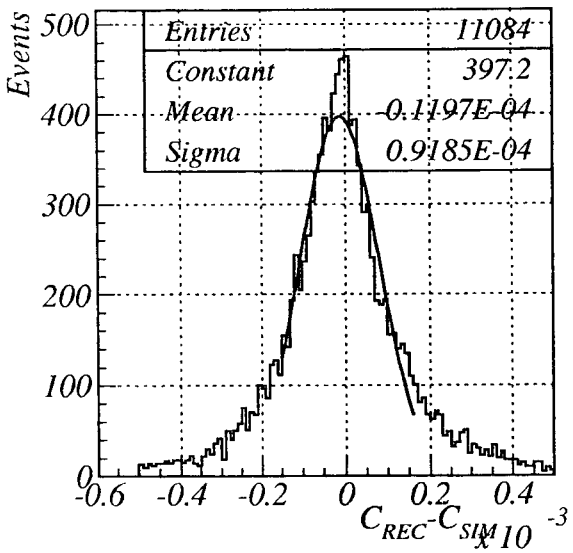

(a) field — 0.4 T

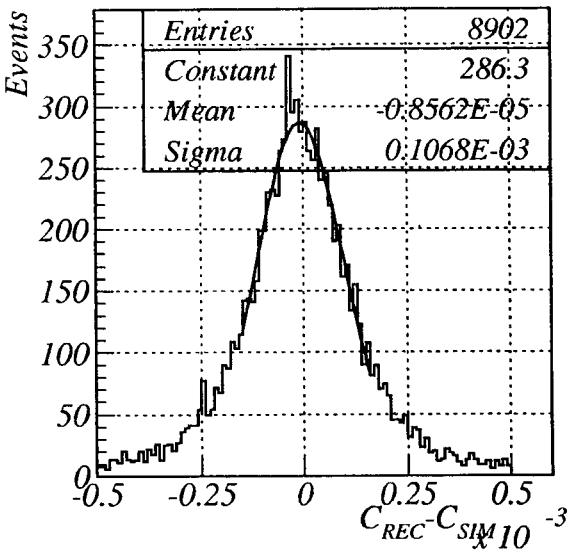

(b) field — 0.1 T

Figure 8: dC spectrum, where dC — difference between reconstructed curvature and simulated one.

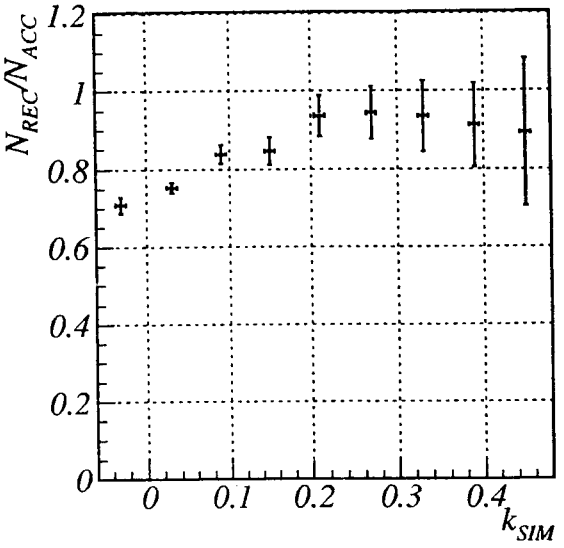

(a) field — 0.4 T

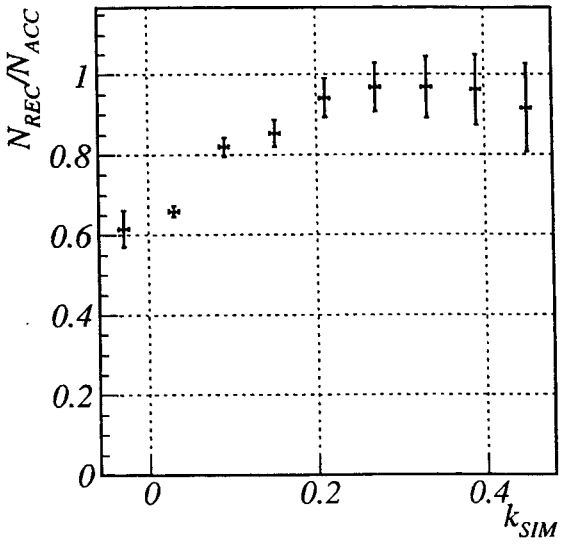

(b) field — 0.1 T

Figure 9: N_{REC}/N_{ACC} dependence on the K parameter in DC2.

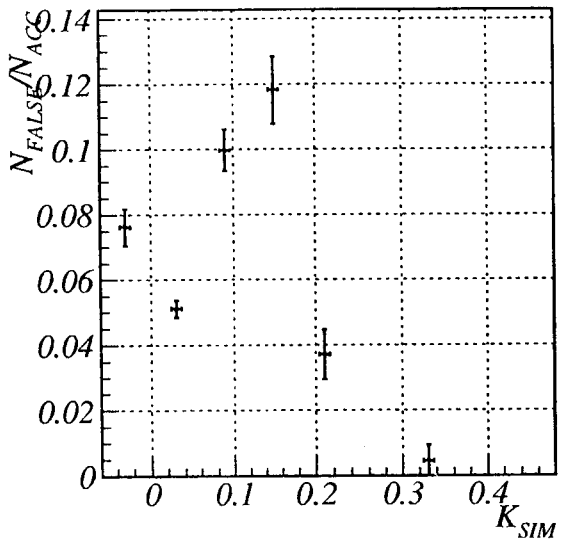

(a) field — 0.4 T

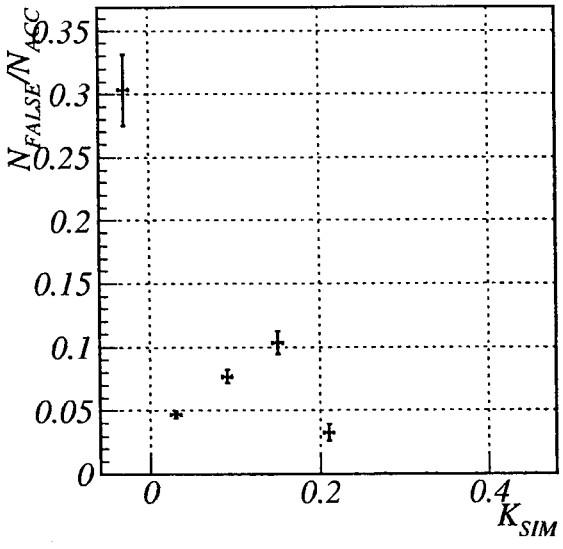

(b) field — 0.1 T

Figure 10: N_{FALSE}/N_{ACC} dependence on the K parameter in DC2..

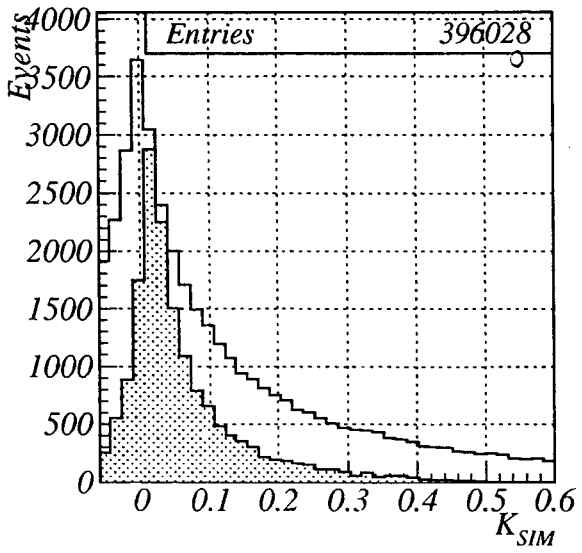

(a) field — 0.4 T

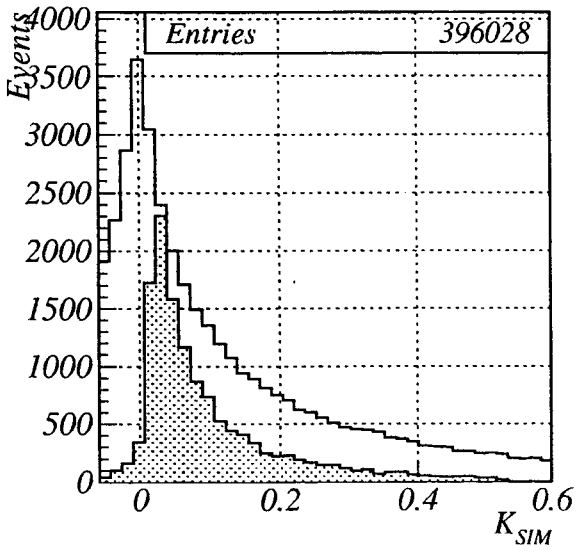

(b) field — 0.1 T

Figure 11: The unfilled histogram is the simulated tracks distribution on parameter K_{SIM} multiplied by the scale factor 0.33 . The gray histogram is the accepted tracks in DC2.

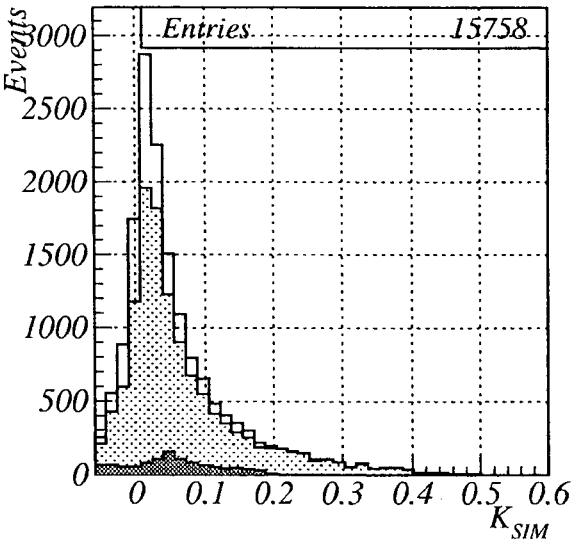

(a) field — 0.4 T

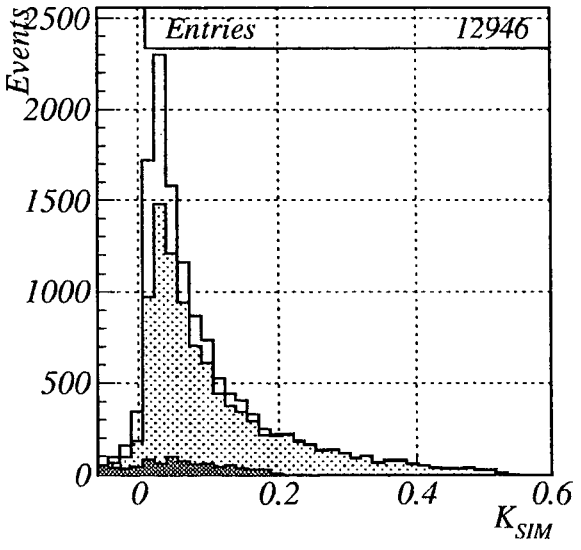

(b) field — 0.1 T

Figure 12: The unfilled histogram is the accepted tracks in DC2. The grey histogram is the correctly reconstructed tracks in DC2. The dark histogram is the false tracks.

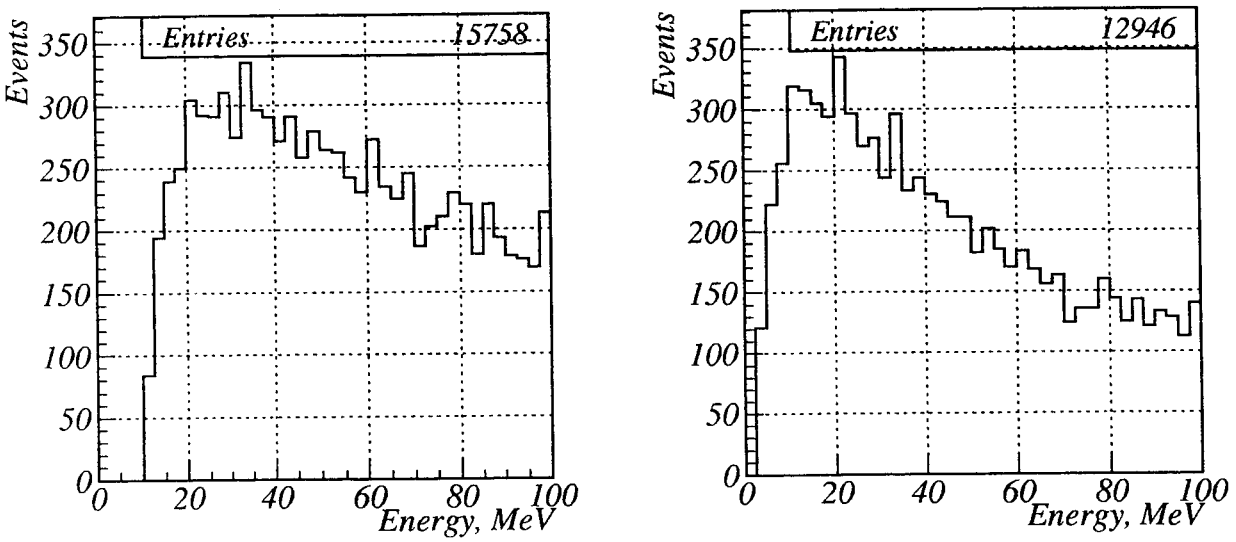

(a) field — 0.4 T

(b) field — 0.1 T

Figure 13: Energy spectrum of accepted particles in DC2.

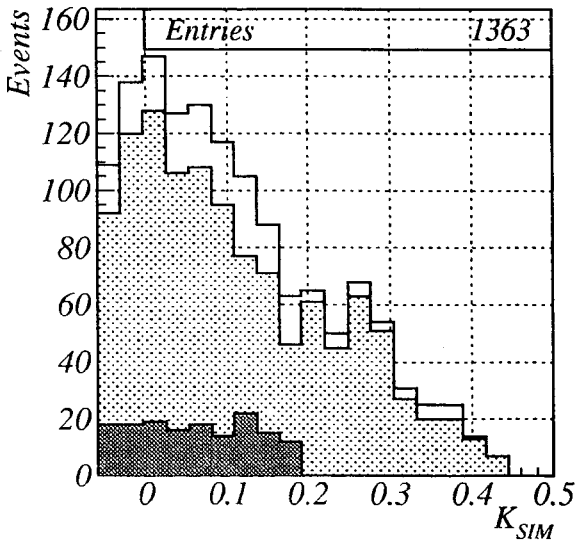

(a) Energy 10–25 MeV

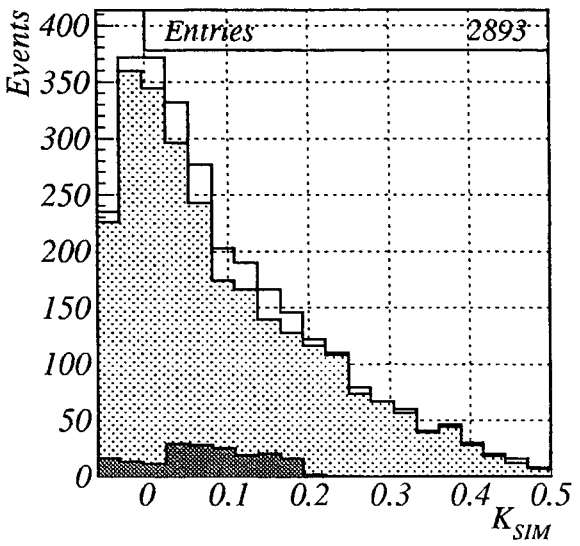

(b) Energy 25–50 MeV

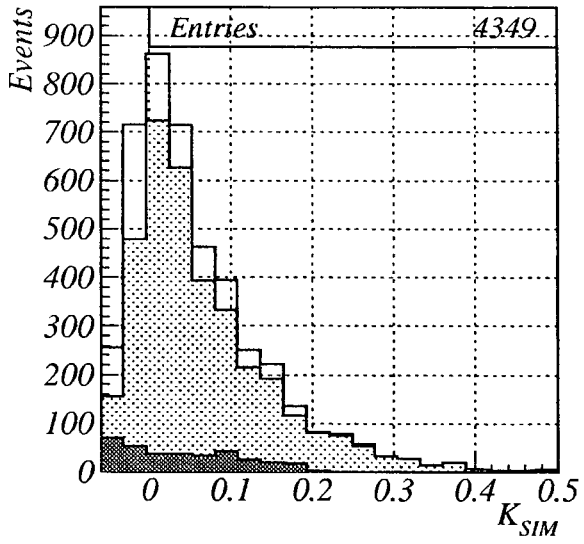

(c) Energy 50–100 MeV

Figure 14: The unfilled histogram is the accepted tracks in DC2. The gray histogram is the correctly reconstructed tracks in DC2. The dark histogram is the false tracks. Field — 0.4 T

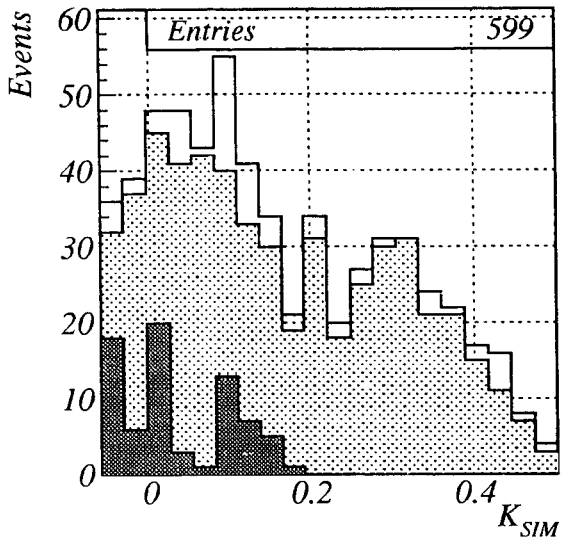

(a) Energy 1–10 MeV

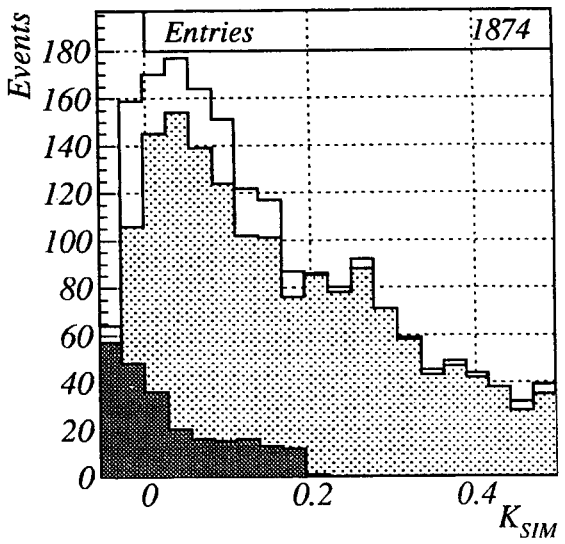

(b) Energy 10–25 MeV

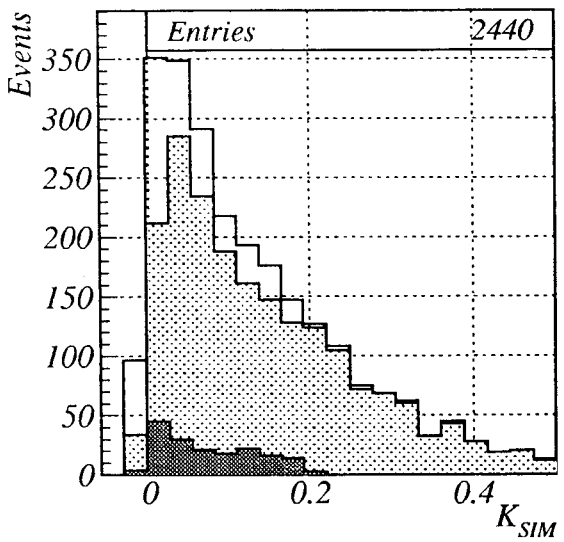

(c) Energy 25–50 MeV

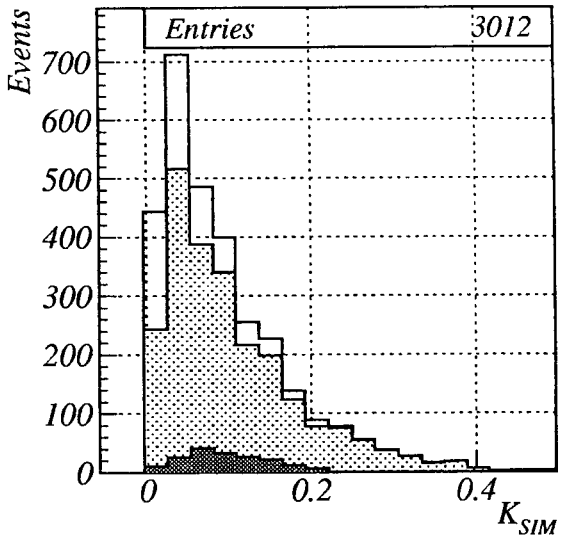

(d) Energy 50–100 MeV

Figure 15: The unfilled histogram is the accepted tracks in DC2. The gray histogram is the correctly reconstructed tracks in DC2. The dark histogram is the false tracks.Field — 0.1 T

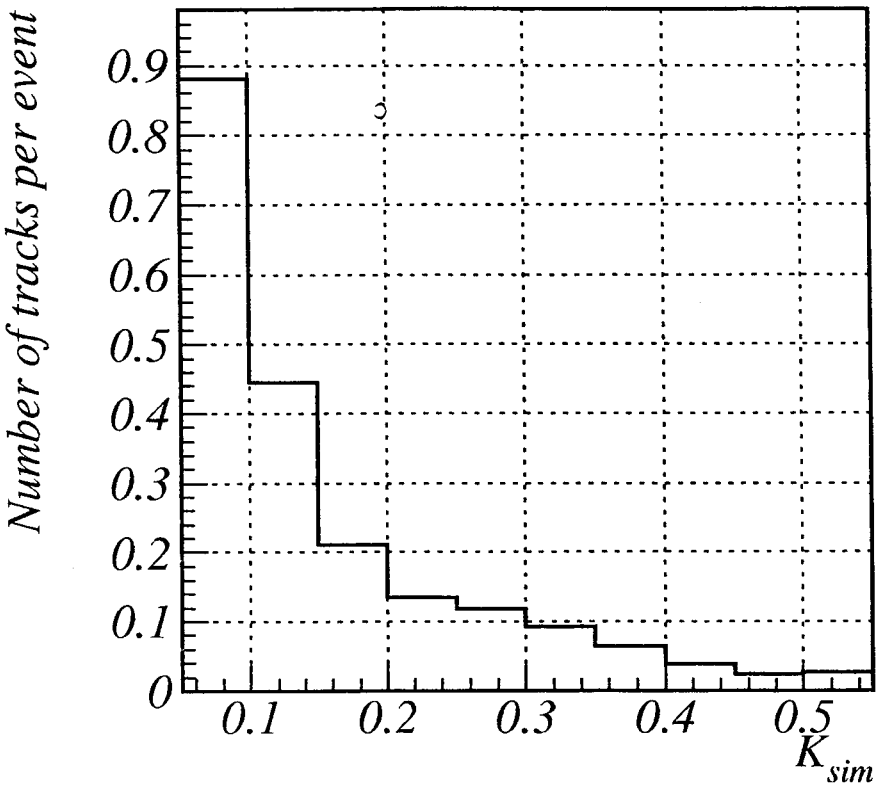

Figure 16: The dependence of the average number of accepted tracks in DC1 per event from K_{SIM} for the amorphous target.

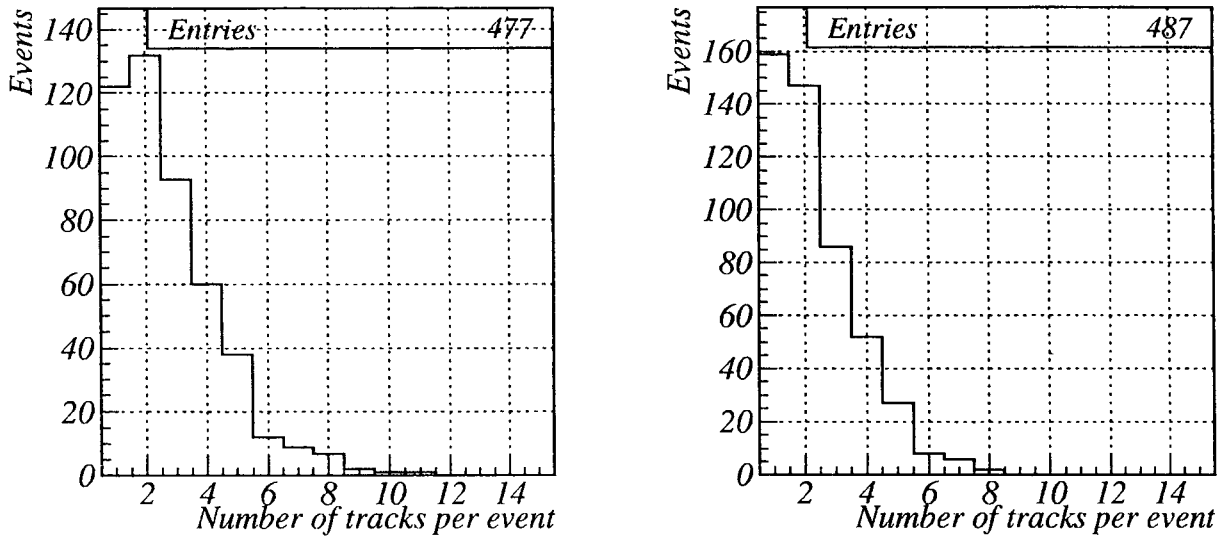

(a) first part

(b) second part

Figure 17: The tracks multiplicity for the amorphous target.

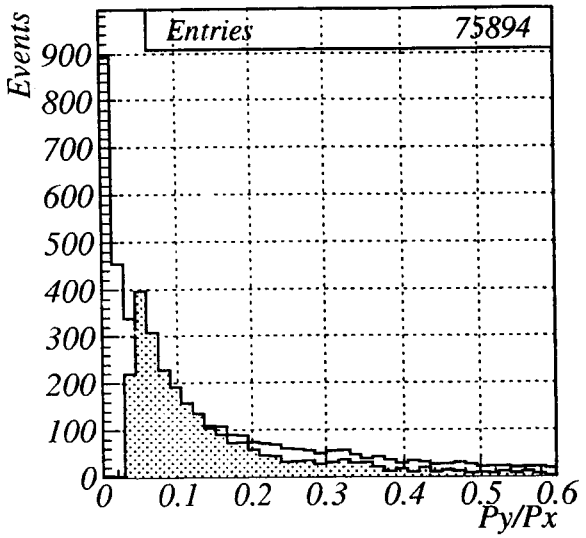

Figure 18: The amorphous target. The unfilled histogram is the simulated tracks distribution on parameter K_{SIM} multiplied by the scaling factor 0.25 . The gray histogram is the accepted tracks in DC1.

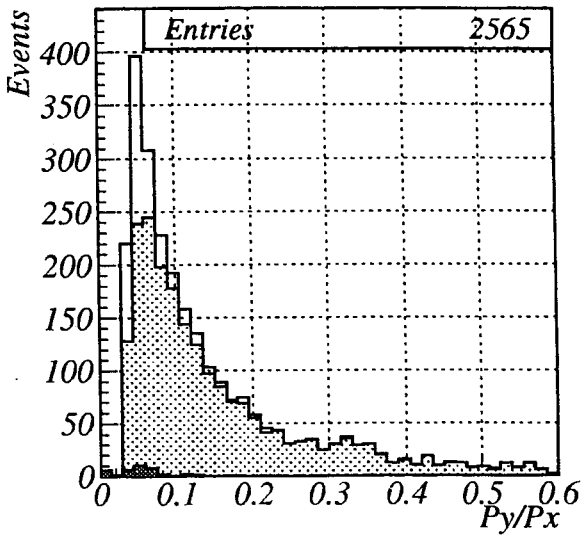

Figure 19: The amorphous target. The unfilled histogram is the accepted tracks distribution on parameter K_{sim} in DC1. The gray histogram is the reconstructed tracks in DC1.The dark histogram is the false tracks in DC1.

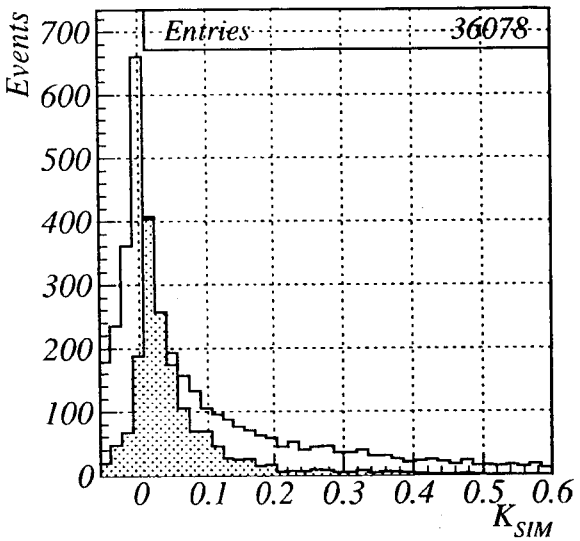

Figure 20: The amorphous target. The unfilled histogram is the simulated track distribution on parameter K_{SIM} multiplied by the scale factor 0.33 . The gray histogram is the accepted tracks in DC2. The field — 0.4 T

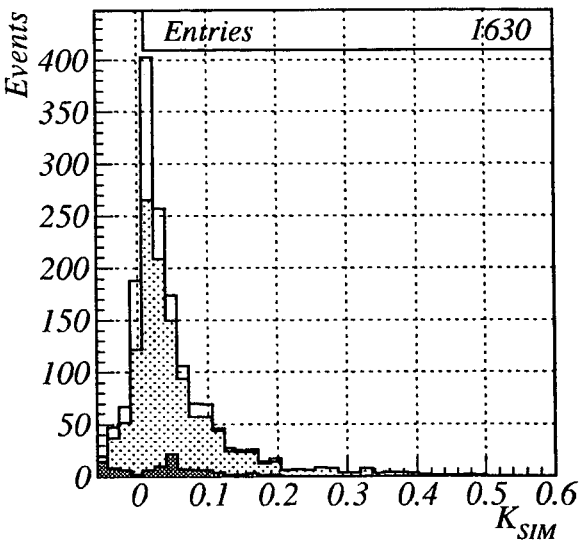

Figure 21: The amorphous target. The unfilled histogram is the accepted tracks in DC2. The gray histogram is the correctly reconstructed tracks in DC2. The dark histogram is the false tracks. The field — 0.4 T.

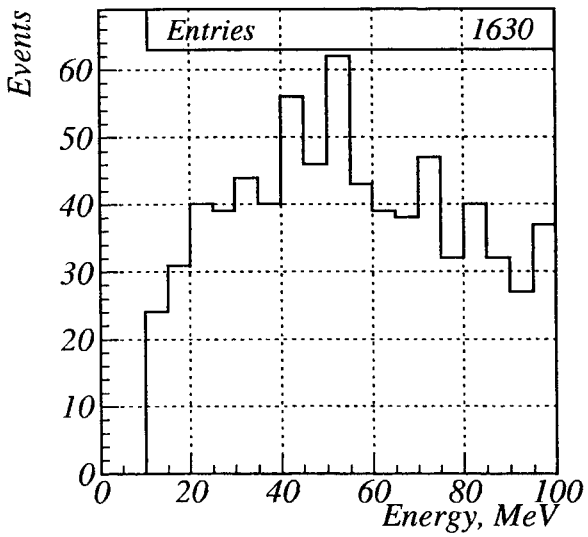

(a) field — 0.4 T

Figure 22: Energy spectrum of accepted particles in DC2 for the amorphous target.

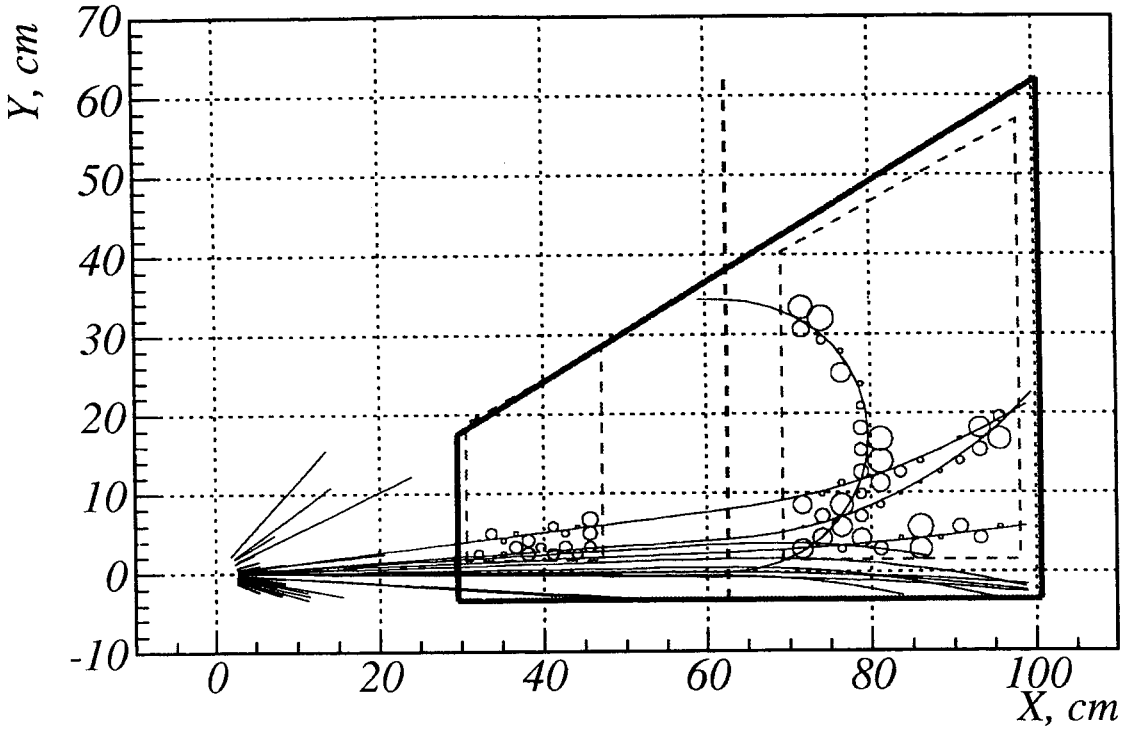

(a) simulated event

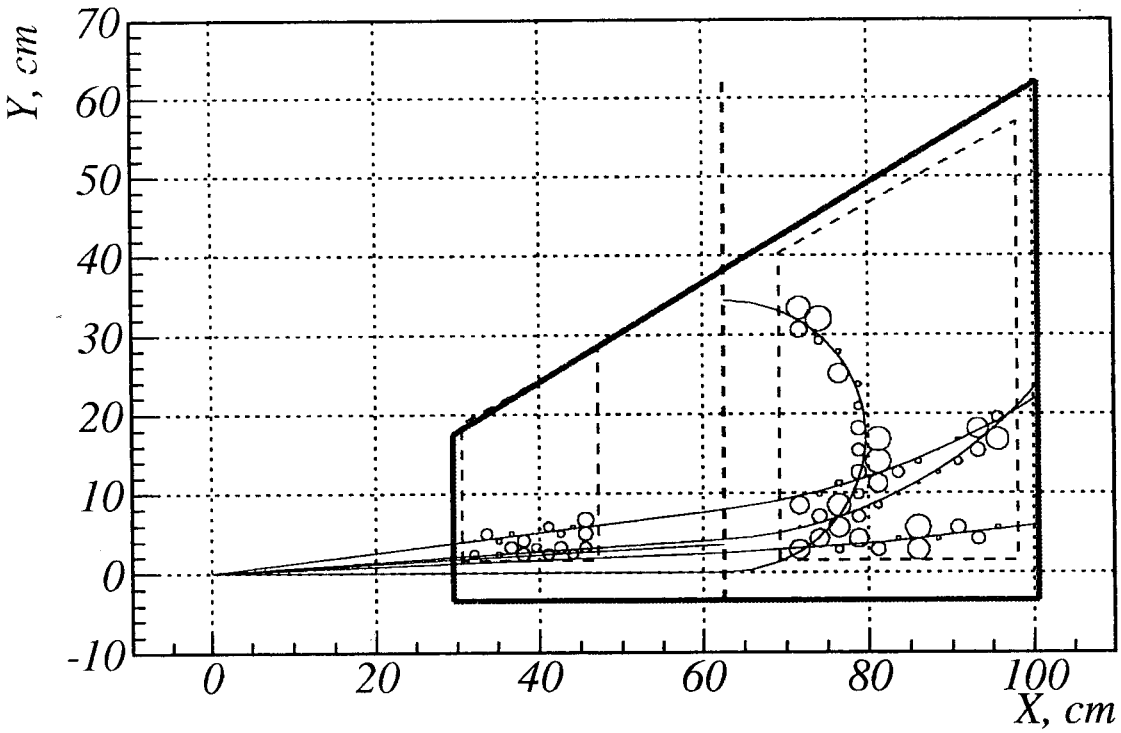

(b) reconstructed event

Figure 23: Event 1. Simulated and reconstructed events. $B = 0.4T$

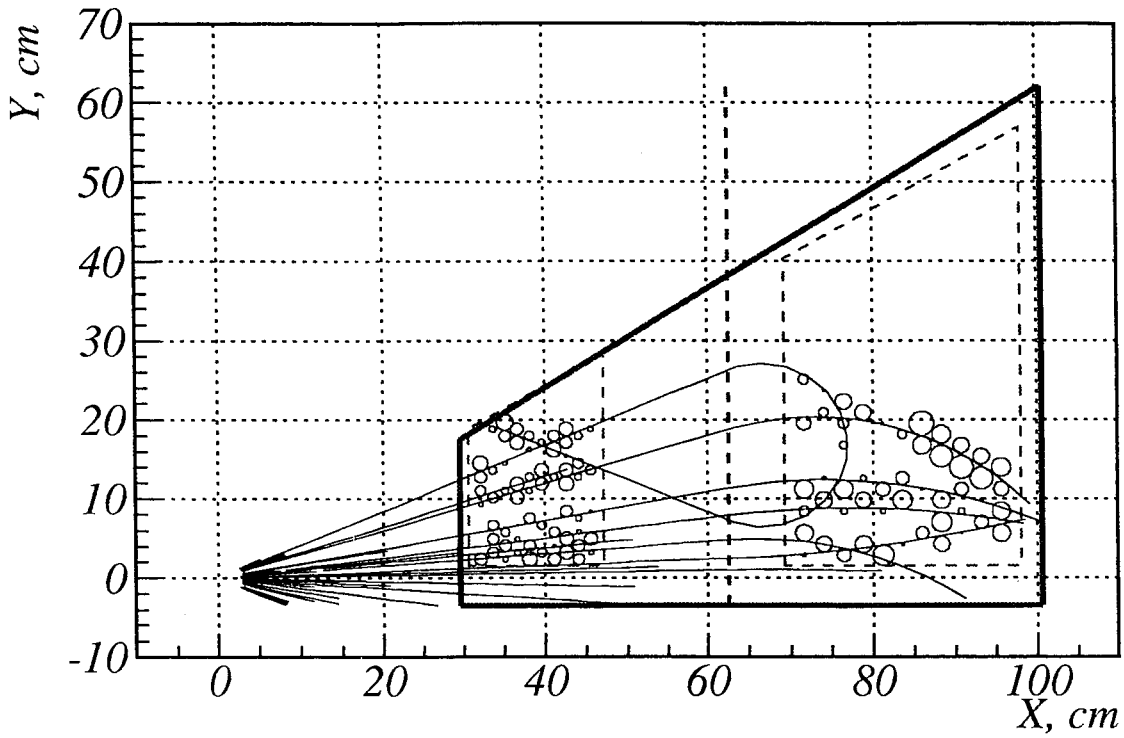

(a) simulated event

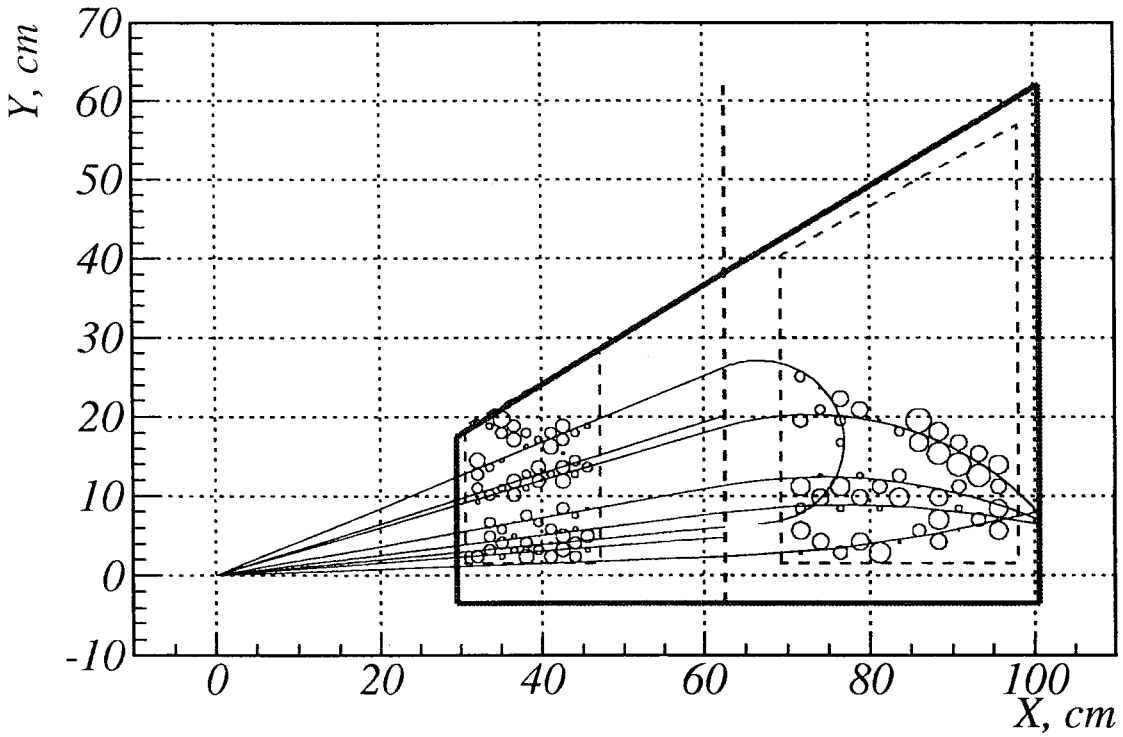

(b) reconstructed event

Figure 24: Event 2. Simulated and reconstructed events. $B = 0.4T$

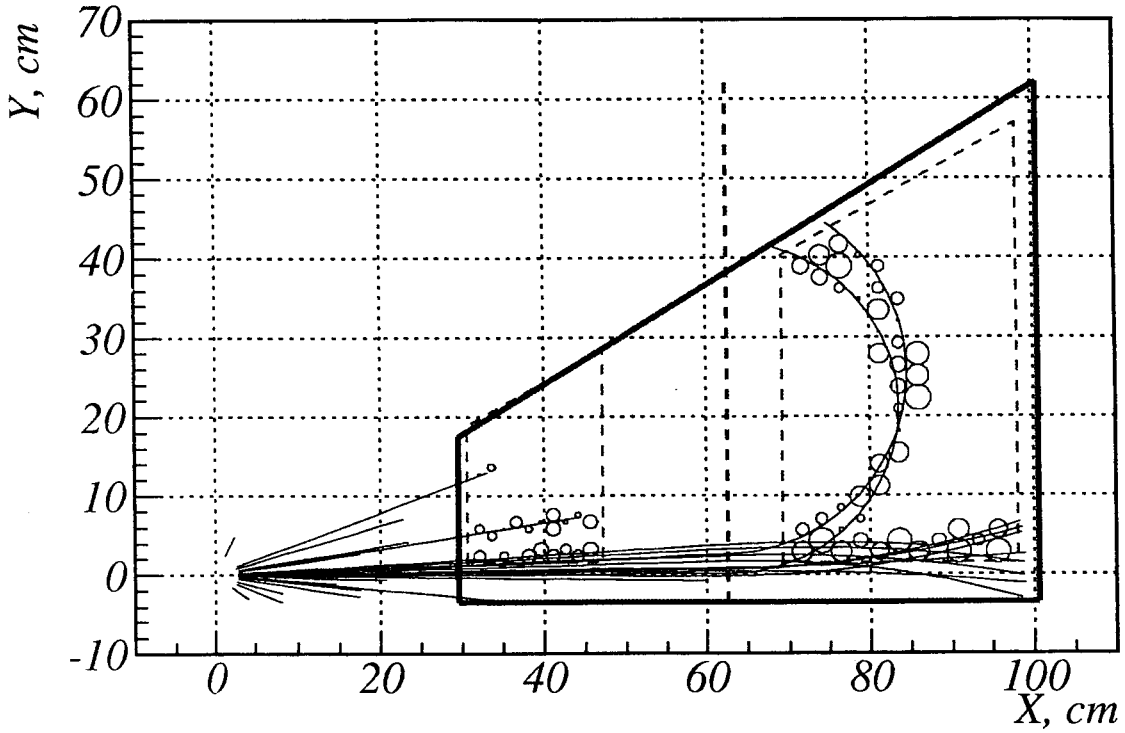

(a) simulated event

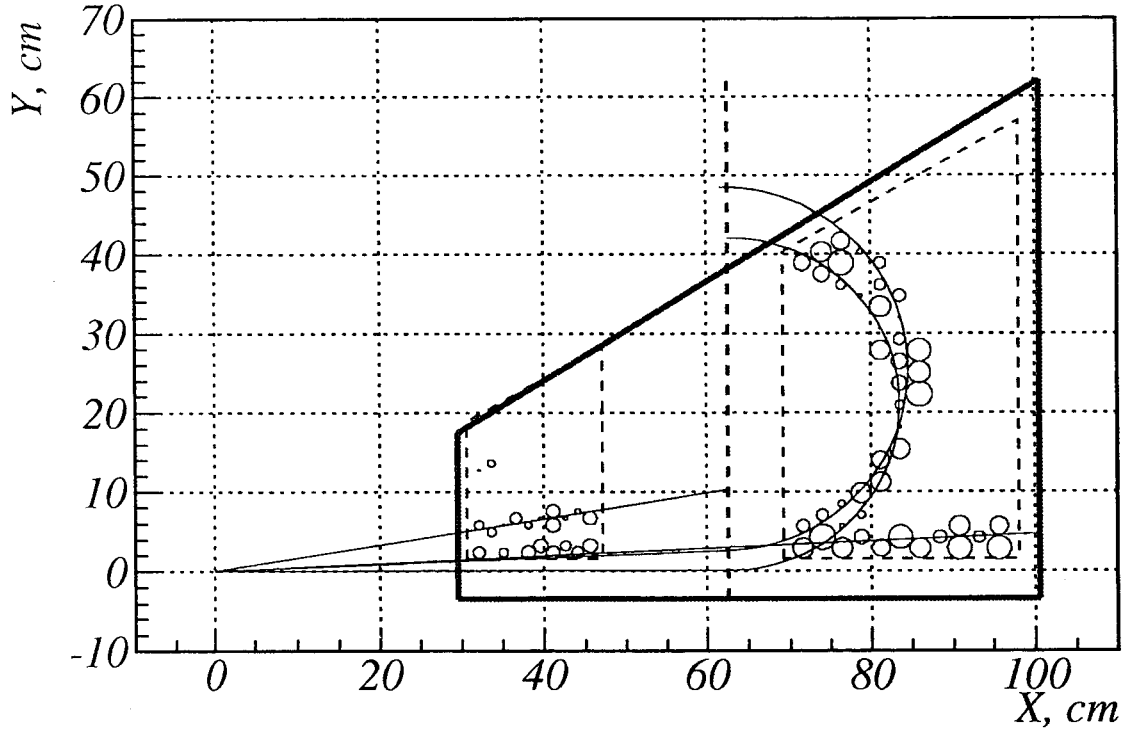

(b) reconstructed event

Figure 25: Event 3. Simulated and reconstructed events. $B = 0.4T$

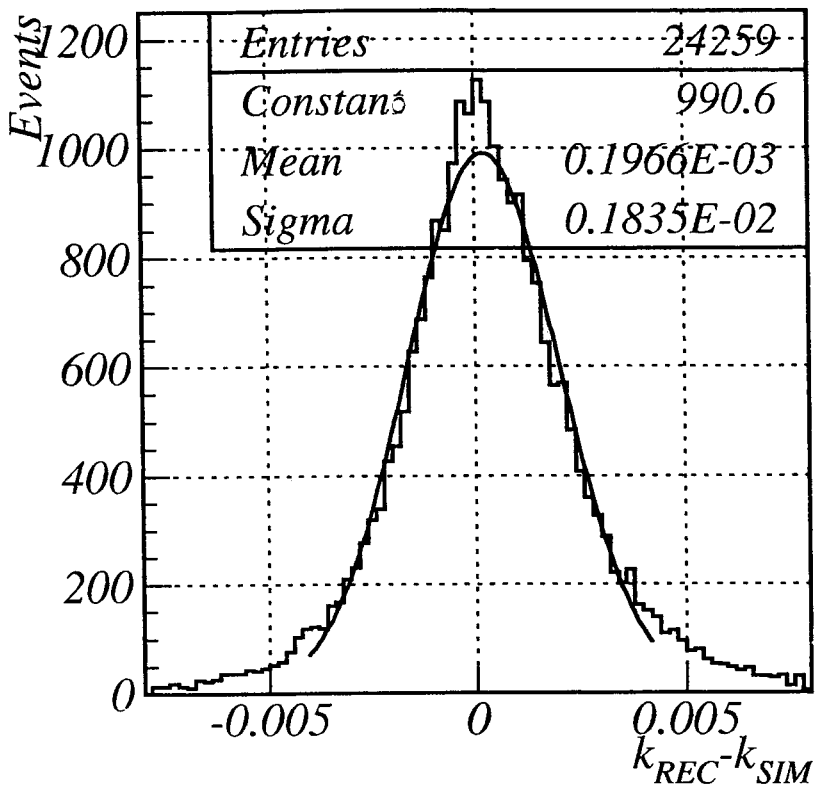

Figure 26: dK spectrum, where dK — difference between reconstructed K_{REC} and simulated one $K_{SIM} = P_Y/P_X$. The beam size is 1 mm.

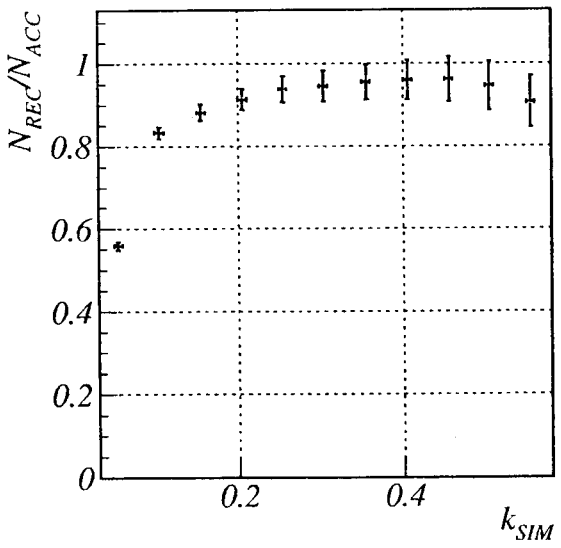

Figure 27: The ratio between reconstructed and accepted tracks in DC1. The beam size is 1 mm.

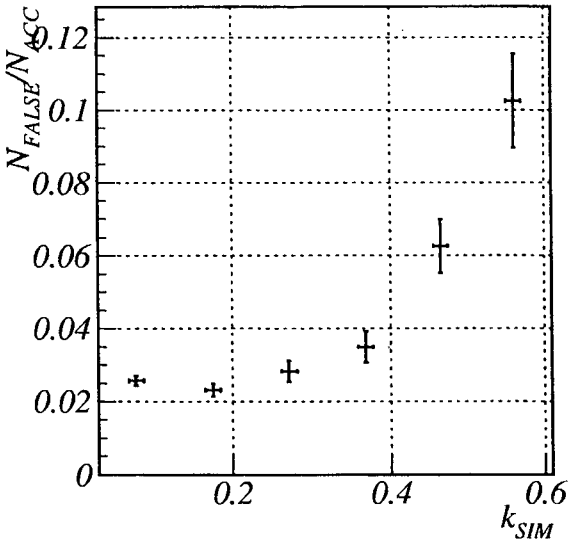

Figure 28: The ratio between false and accepted tracks in DC1. The beam size is 1 mm.

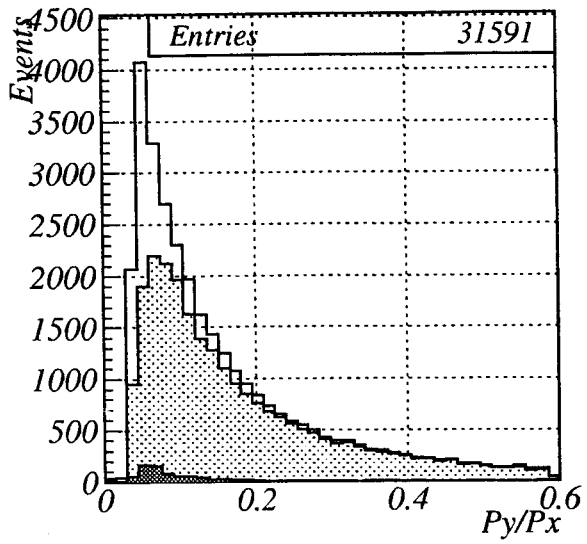

Figure 29: The unfilled histogram is the accepted tracks distribution on parameter K_{sim} in DC1. The gray histogram is the reconstructed tracks in DC1.The dark histogram is the false tracks in DC1. The beam size is 1 mm.

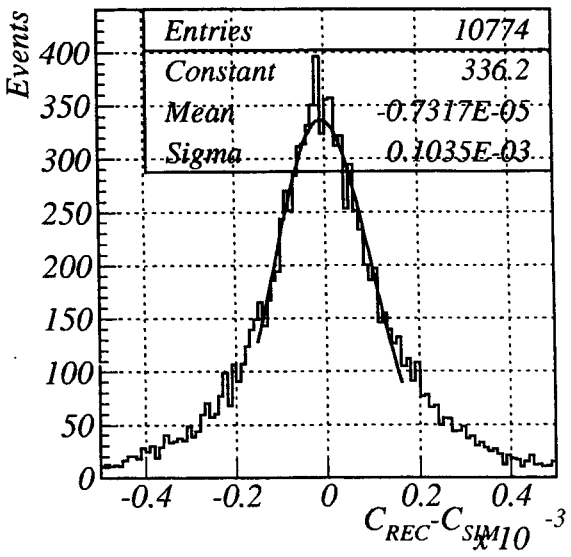

Figure 30: dC spectrum, where dC — difference between reconstructed curvature and simulated one. Field — 0.4 T. The beam size is 1 mm.

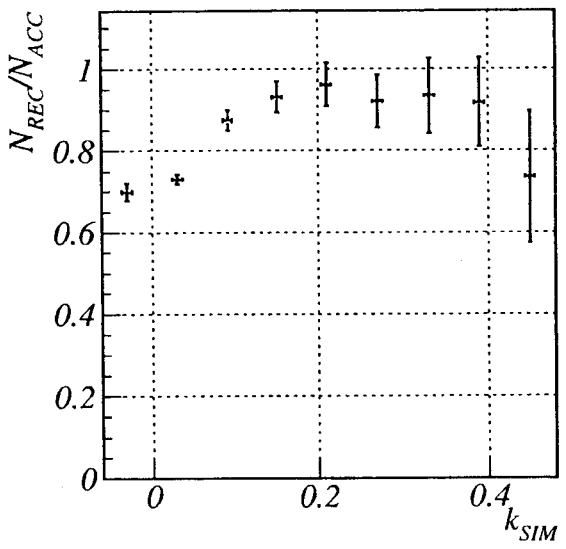

Figure 31: N_{REC}/N_{ACC} dependence on the K parameter in DC2. Field — 0.4 T. The beam size is 1 mm.

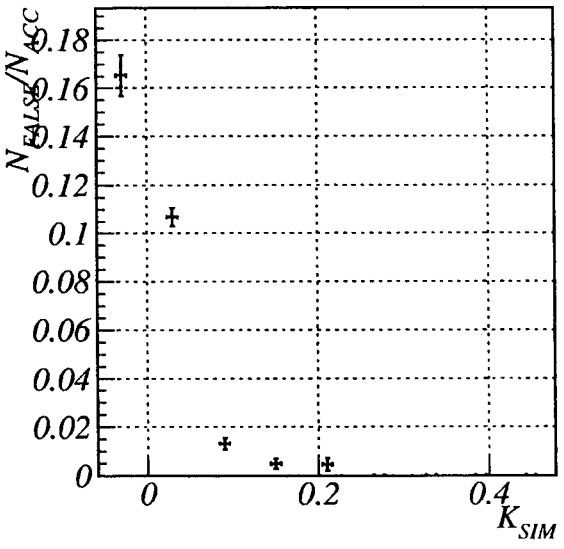

Figure 32: N_{FALSE}/N_{ACC} dependence on the K parameter in DC2. Field — 0.4 T. The beam size is 1mm.

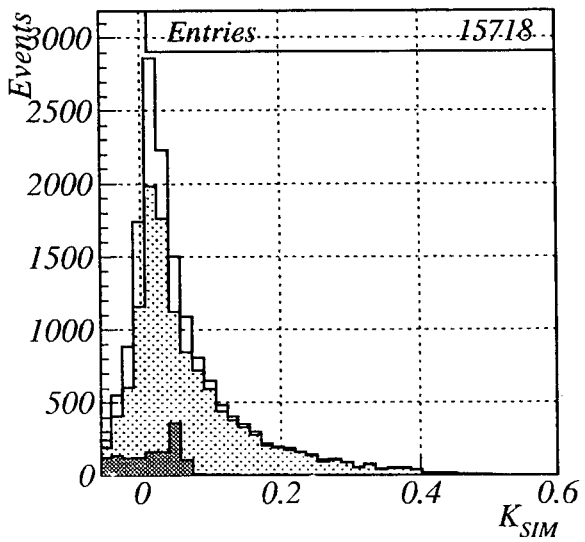

Figure 33: The unfilled histogram is the accepted tracks in DC2. The gray histogram is the correctly reconstructed tracks in DC2. The dark histogram is the false tracks. Field — 0.4 T. The beam size is 1 mm.

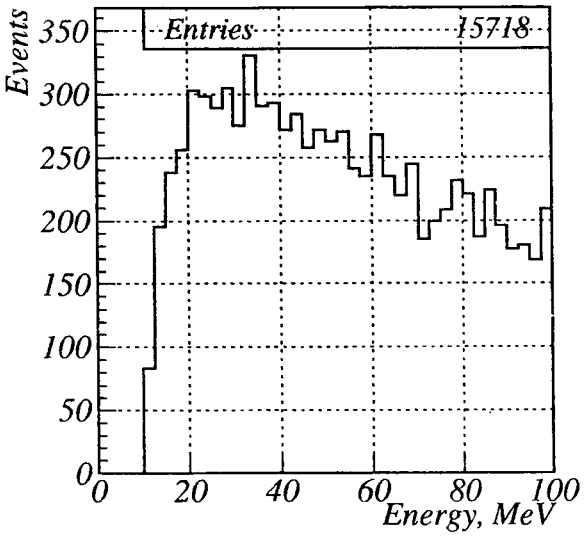

Figure 34: Energy spectrum of accepted particles in DC2. Field — 0.4 T. The beam size is 1 mm.

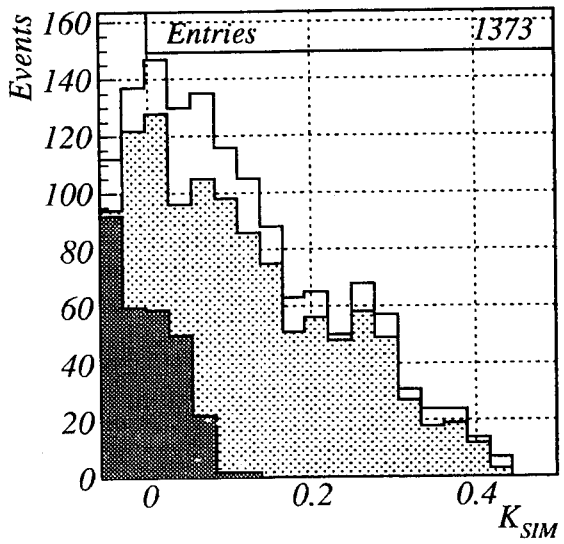

(a) Energy 10–25 MeV

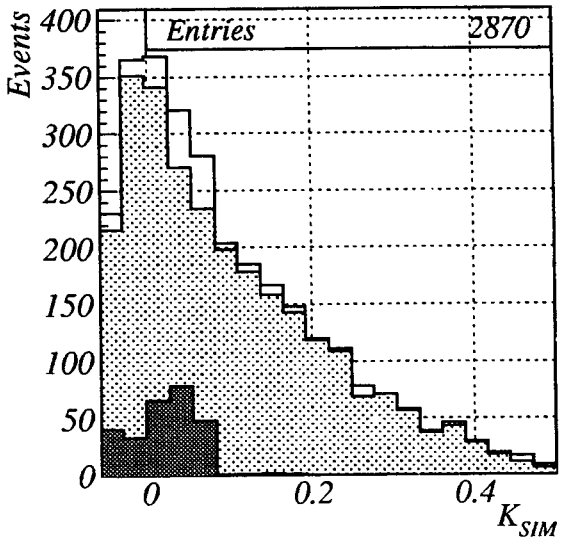

(b) Energy 25–50 MeV

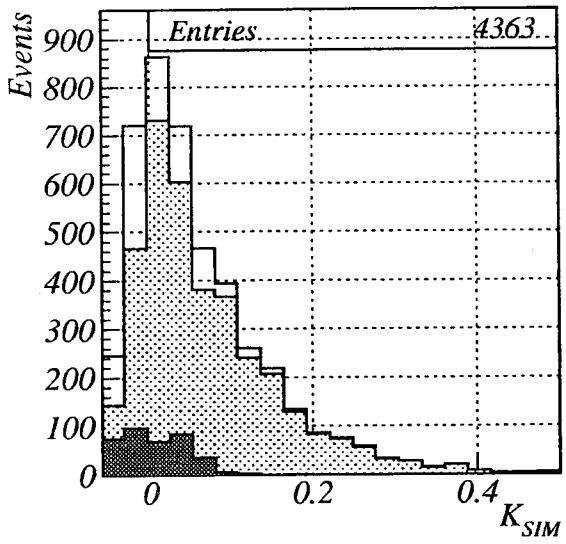

(c) Energy 50–100 MeV

Figure 35: The unfilled histogram is the accepted tracks in DC2. The gray histogram is the correctly reconstructed tracks in DC2. The dark histogram is the false tracks.Field — 0.4 T. The beam size is 1 mm.